CORROSION SCIENCE AND TECHNOLOGY, Vol.21, No.2(2022), pp.121~129 pISSN 1598-6462 / eISSN 2288-6524
[Research Paper] DOI: https://doi.org/10.14773/cst.2022.21.2.121

# Optimization of Process Parameters for Dry Film Thickness to Achieve Superior Water-based Coating in Automotive Industries

**Pranay Kant Prasad[1], Abhinav Kr Singh[2], Sandeep Singh[3], Shailesh Kumar Prasad[1], and Sudhanshu Shekher Pati[1,†]**

[1]*Department of Chemistry, NIT Jamshedpur, Jharkhand, India-831014*
[2]*Tata Motors, Jamshedpur, Jharkhand, India-831014*
[3]*Department of Mechanical Engineering, NERIST, Arunachal Pradesh-791109*
(Received January 09; Revised February 10, 2022; Accepted February 14, 2022)

A study on water-based epoxy coated on mild steel using the electroplating method was conducted to optimize the process parameters for dry film thickness to achieve superior paint quality at optimal cost in an automotive plant. The regression model was used to adjust various parameters such as electrode voltage, bath temperature, processing time, non-volatile matter, and surface area to optimize the dry film thickness. The average dry film thickness computed using the model was in the range of 15 – 35 μm. The error in the computed dry film thickness with reference to the experimentally measured dry film thickness value was -0.5809%, which was well within the acceptable limits of all paint shop standards. Our study showed that the dry film thickness on mild steel was more sensitive to electrode voltage and bath temperature than processing time. Further, the presence of non-volatile matter was found to have the maximum impact on dry film thickness.

***Keywords:*** *Surface coating, Regression model, Automobile painting, Dry film thickness, Paint process parameter*

## 1. Introduction

Considering the size of the automobile industry worldwide, any possible reduction in production cost has been a topic of intense research for decades. For instance, the painting cost (approximately Rs.13.5/$m^2$ for the Cathodic Electrode Deposition (CED)) has significant contribution to the total cost of a bare chassis of a commercial vehicle which is about 90 $m^2$ of a bare chassis with driver's cab. Since the volumes produced annually is very high, this translates to a huge expenditure on paint as raw material. Besides cost, optimizing the durability of exterior coatings considered to be one of the major challenges faced in automobile industries. Although aesthetics is an important aspect of the surface paint, the primary duty of the CED paints in an automobile chassis is to protect the underlying structure from the atmosphere which is crucial from corrosion point of view. Several studies have been pursued to improve the corrosion and degradation resistance by selective surface modification [1-3]. To improve deep-draw processing performance and formability of precoated metal sheets, Lee *et al.* developed phosphoric acid-functionalized acrylic polyol based clearcoats for automotive applications [2]. Inorganic-organic based nanocomposite coating material synthesized using a sol-gel method showed better control of size, periodicity, spatial positioning and density of the inorganic phase[4]. Cliff *et al.* tried to improve durability of the coating in presence of ultra-violet radiations which otherwise migrate out of the topcoat to the underlying plastic substrate [1]. However, Optimizing the cost is still a challenge even though researcher have succeeded in improving the corrosion resistance.

The most challenging task a process engineer faces in the automotive industry is to improve the efficiency of the manufacturing processes without compromising the cost in view of the global competition in which the company must survive. Consistent quality, higher production, lowered costs, social responsibility, environmental and workplace safety are some of the parameters which are often optimized for any industrial painting process. Optimizing any of the above factors require readjustment

†Corresponding author: sspati.chem@nitjsr.ac.in

in all parameters to obtain optimal relationship among them leading to high quality at reasonable cost. For the paint shop engineers, cost savings in terms of low raw material consumption is a major concern because it directly impacts the profit margins, reliability and environmental issues such as oxide mixed effluent disposal to storm water.

Automobile manufacturing and assembly may be categorized into three different sections i.e construction of fairing, painting operations and final assembly [5]. The painting operation is carried out in three steps namely pretreatment, application, drying and curing. For creation of a docile surface to host and bind the paint, phosphating is the most common pretreatment, where body?in?white (BIW) of the vehicle is cleaned and coated with phosphate solution [6], with few exceptions like zirconium-based conversion coatings [7] in the pretreatment process. Comparative studies of various pretreatment materials along with its environmental impact has been thoroughly summarized by Doerre *et al*. [8] Reports suggest that zirconium oxide conversion coatings has sludge reduction as high as 95% over tri-cationic phosphating at ambient temperature which leads to reduction in energy consumption and low toxicity [9]. Also, $ZrO_2$ has a higher Al surface area without detrimental effects in automotive bodies in compared to other existing pretreatment methods. It has been reported that fused epoxy and conducting polyaniline-based paints exhibits insignificant iron loss of ~0.06 ppm in NaCl solution when exposed to impressed current cathodic protection [10]. These conducting polyaniline-based paint were promising to protect low carbon steel in neutral medium. In a recent study on coating of an enamel layer to increase the corrosion behavior of aluminum foam shows high increase of corrosion behavior when compared with uncoated aluminum foam [11].

Spray painting operations are widely used in automotive industry. However, eliminating or minimizing the extent of spray application processes including baking in ovens can result in substantial cost benefits on account of material and energy [12]. Cavalcante et. al. reported that his proposed methodology has potential to develop operational optimization strategies which can reduce rework and energy costs deprived of compromising painting quality [13]. Industrially applied CED process for painting is usually an integrated version of the laboratory established procedures considering growing competitiveness and operational limitations. The foremost difference exists in the flexibility of selecting the equipment and fixing the process parameters for individual components. In a jobbing CED paint shop, individual component has the flexibility to allot unique time slot and unique process parameters; however, in production line associated CED shop, multiple component combinations of different surface areas may be processed, with the given set of equipment and paint parameters. Different surface area of components when processed with same set of parameters results in variation of dry film thickness (DFT) [14]. DFT is a very sensitive parameter as a lower value of DFT is considered as quality deficiency and a higher value of DFT can increase the painting cost substantially. To optimize the DFT to obtain paint which maximizes the quality of the automobile without increasing the cost significantly, fixing the process parameters is of great importance.

The paint quality by electroplating depends on current density, stirring rate and bath temperature which give rise to different properties of the deposited film [15]. It has been reported that solubility of metal ions in the electrolyte increases with increase in bath temperature which results in reduction of the viscosity and increases the transport number and conductivity of the solution [16]. Again, higher bath operating temperature reduces the tendency towards cracking due to hydrogen induced stress by reducing hydrogen intake of the metal and substrate. Balaji et al. reported that incorporation of polytetrafluoroethylene particles during electrodeposition of bronze– polytetra-fluoroethylene composite coatings has higher incorporation rate in sediment co-deposition technique than conventional electrodeposition technique [17]. Owing to the complexity of optimization, regression based models have been frequently employed in studying the properties of deposited coatings such as prediction of hardness and volume percent of diamond in Ni–diamond composite coatings [16,18].

The present work envisions to understand the effect of various process parameters including the component geometry on the DFT in a typical CED process. The experimental part aims to correlate the influence of Electrode Potential (V), Bath Temperature (T), fraction of Non-Volatile Matter in the bath solution (%NVM), Process time (t) and job surface area (A) on the final Dry

Film Thickness (DFT). A simplified model based on linear regression has been developed for identification of all the above-mentioned participation coefficients. The developed model can be used to optimize the process parameters which not only reduces the cost but also saves a lot of time. The algorithm developed for this purpose has been tested for robustness by adding 1%, 2% and 5% random noise (Gaussian White Noise) to the measured parameters and the results with noise adulterated data is presented in this work.

## 2. Experimental Section

### 2.1 Set up and Method

A water-based paint was used for the present study using epoxy as the electrolyte. Fig. 1a represents the schematic of the electrochemical reaction set up and Fig. 1b depicts the electrodeposition setup used for coating which consists of one anode (stainless steel), a cathode made of mild steel, a magnetic stirrer, current generators (rectifiers), speed and temperature control device. The chemicals ($CH_3COOH$, Polymer-$NR_2$) used for this work were procured from SRL chemicals limited and used without any further purification.

The composition of the bath used for the electro-deposition are as follows.

$$\text{Polymer-NR}_2 + \text{H}_3\text{C-COOH} \rightarrow \text{Polymer-N+R}_2\text{H} + \text{H}_3\text{C-COO}^-$$

$$\text{Polymer-N+R}_2\text{H} + \text{OH}^- \rightarrow \text{Polymer-NR}_2 \downarrow + \text{H}_2\text{O}$$

The distance between anode and cathode was 7 cm. The coating area was 116 $cm^2$. The operating temperature was maintained in the range of Temp-30 ºC to 32 ºC and the pH of the electrolyte was varied from 5.5 to 6.1. The voltage was varied from 230 to 340 V in which the electrodeposition parameters were optimized by tuning the bath temperature from 30 to 35 ºC, nonvolatile matter

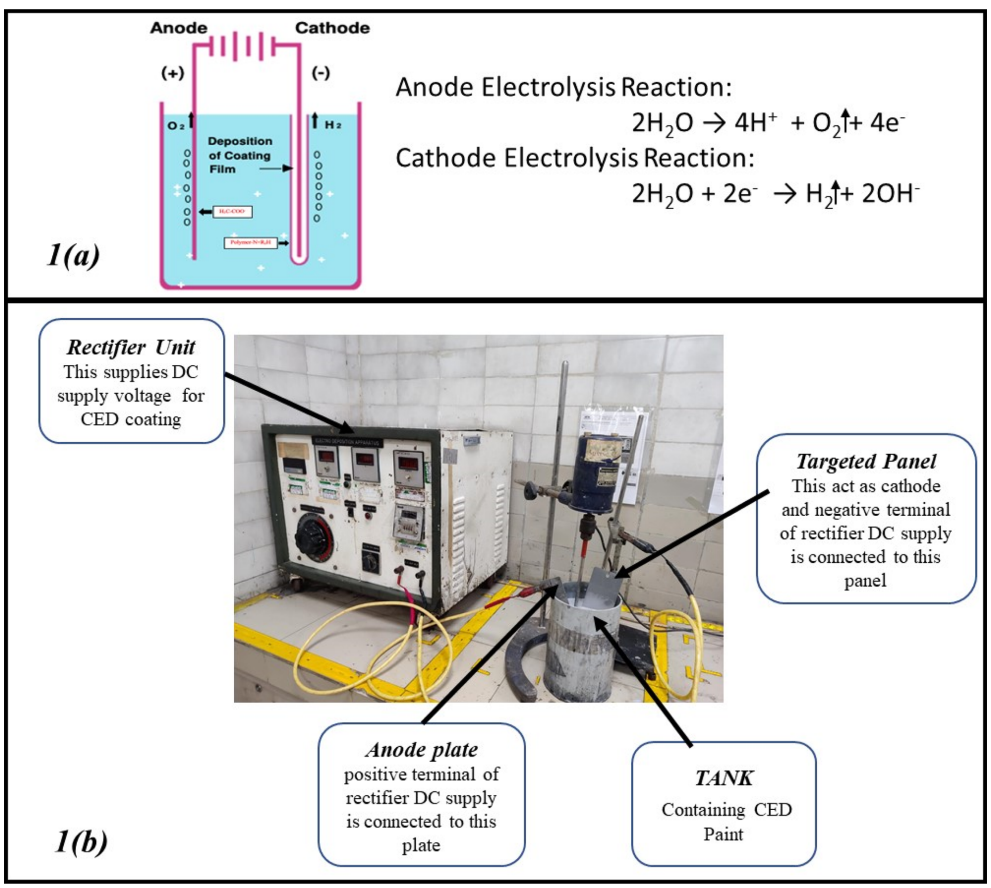


**Fig. 1. (a) schematic of electrochemical reaction set up and (b)The complete Cathode Electrodeposition (CED) Setup used for application of prepared water-based paint on targeted material**

from 13 to 17%, process time from 120 to 180 secs and surface area from 116 sq. cm to 258 sq. cm. All the experiments were conducted in quality lab facility of Paint Shop, Tata Motors Ltd, Jamshedpur. Figure I and Figure II represent the electrodeposition set up and electrodeposition panels used for the work, respectively.

### 2.2 Result

The experimental study intends to correlate the various process parameters and their cohesive impact on the dry film thickness of the CED paint. For each observation, only one parameter has been varied keeping the other four constant in the range of interest. Repetitive measurements

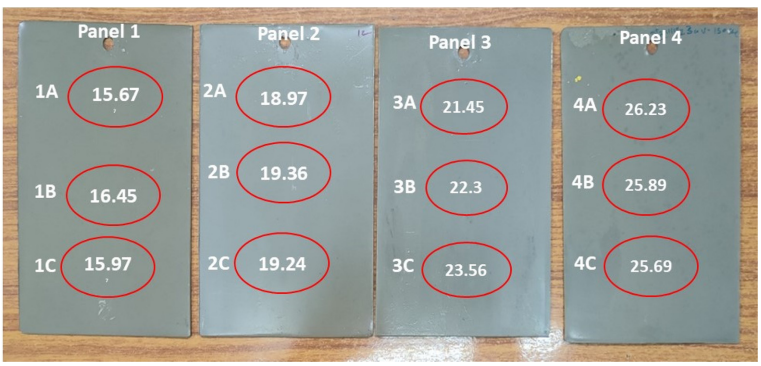


**Fig. 2. Representative points on the electrodeposited panels used for the calculation of dry film thickness**

**Table 1. Average Dry Film Thickness (DFT) at different parameter values**

| Variable Parameter | Variable Parameter values | Units | Fixed Parameter Values | Average DFT (μm) |
|---|---|---|---|---|
| Electrode Voltage | 230 | Volts | %NVM: 15.27 Temperature: 31.2 °C Process time: 150 sec. | 15.55 |
| | 250 | | | 17.22 |
| | 280 | | | 19.52 |
| | 300 | | | 22.26 |
| | 320 | | | 28.22 |
| | 340 | | | 35.6 |
| Bath Temperature | 30 | °C | % NVM: 15.25 Voltage: 280 Volts Process Time: 150 sec. | 18.17 |
| | 31 | | | 19.93 |
| | 32 | | | 22.15 |
| | 33 | | | 23.51 |
| | 34 | | | 25.58 |
| | 35 | | | 28.5 |
| % NVM | 13 | % | Temperature: 30 °C Voltage: 280 Volts Process Time: 150 sec. | 16.9 |
| | 14 | | | 17.05 |
| | 15 | | | 19.43 |
| | 16 | | | 20.77 |
| | 17 | | | 24.39 |
| Process Time | 120 | seconds | Temperature: 30 °C Voltage: 280 Volts % NVM: 15.21 | 16.44 |
| | 140 | | | 17.93 |
| | 160 | | | 20.32 |
| | 180 | | | 23.23 |
| Surface Area | 4×10 | Square inch | Temperature: 30 °C Voltage: 280 Volts % NVM: 15.22 | 23.26 |
| | 5×6 | | | 25.3 |
| | 5×3 | | | 27.74 |
| | 3×6 | | | 25.98 |

were carried out for each of the parameters. Every experimental parameter set is associated with ten DFT values. The complete data of DFT obtained from the experimental CED on panels is placed in data repository and the average of the results obtained for DFT has been reported in the present work. The summary of averaged out data is presented in Table 1.

## 3. Theoretical Studies

### 3.1 Identification of Algorithm

The experimental study presented in this work has 5 operating variables i.e., Electrode Voltage ($V$), Bath Temperature ($\theta$), % NVM ($\rho$), Process Time ($t$) and Surface Area ($A$), which controls the DFT of the paint. As presented in Table 1, we can derive that electrode voltage, bath temperature, NVM concentration and process time have direct proportionality with DFT whereas the surface area of the specimen has negative impact on the DFT. Therefore, a computational modelling of the process parameters was undertaken to optimize DFT in the range of 16 to 23 μm which can save a lot of time and cost. Based on the number of variables, it is intuitive to assume a relationship of the form

$$\alpha_1 V + \alpha_2 \theta + \alpha_3 \rho + \alpha_4 t + \alpha_5 A = DFT \quad (1)$$

The signs of these coefficients $\alpha_1$ through $\alpha_5$ may be positive or negative due to complex interaction of the 5 operating parameters being investigated, depending upon the chemistry of the individual parameter. The first 4 parameters are expected to have positive coefficients and the 5$^{th}$ parameter is expected to have negative coefficient, based on the experimental intuition. To obtain the values of the coefficients $\alpha_1$ through $\alpha_5$, the data presented in Table 1 are written in the form of equation (1), for instance, the first and the last data series of Table 1 is written as:

$$230\alpha_1 + 31.2\alpha_2 + 15.27\alpha_3 + 150\alpha_4 + 48\alpha_5 = 15.55 \quad (2)$$

$$280\alpha_1 + 30\alpha_2 + 15.22\alpha_3 + 150\alpha_4 + 18\alpha_5 = 25.98 \quad (3)$$

All other data series are written accordingly. It is notable here that Table 1 presents only the DFT which is average of a few observations at a particular operating parameter set; the true data available is nearly 5 times larger than that reported in the paper. The complete data is available in repository indicated. All other data sets are converted to the form indicated in equation (1) and thus there are 25 equations of form $\alpha_1 V + \alpha_2 \theta + \alpha_3 \rho + \alpha_4 t + \alpha_5 A = DFT$ with 5 unknowns viz. $\alpha_1$ through $\alpha_5$. For determination of these 5 unknowns, the 25 equations based on the 25 data sets are converted to the matrix form as:

$$\begin{bmatrix} 230 & 31.2 & 15.27 & 150 & 48 \\ & \ddots & & & \\ & & \ddots & & \\ & & & \ddots & \\ 280 & 30 & 15.27 & 150 & 18 \end{bmatrix}_{25\times5} \begin{Bmatrix} \alpha_1 \\ \alpha_2 \\ \alpha_3 \\ \alpha_4 \\ \alpha_5 \end{Bmatrix}_{5\times1} = \begin{Bmatrix} 15.55 \\ \vdots \\ \vdots \\ \vdots \\ 25.98 \end{Bmatrix}_{25\times1} \quad (4)$$

which is in the standard matrix form

$$Ax = b \quad (5)$$

Since there are 25 equations and only 5 unknowns, it constitutes an overdetermined matrix system. The matrix equation (4) can be solved by converting the rectangular matrix A to its pseudo-square form by least square regression as:

$$x = (A^T A)^{-1} A^T b \quad (6)$$

### 3.2 Results and Discussion

To implement the least square regression to solve the matrix equations as in equation (6), a Matlab® code is implemented, and the values for $\alpha_1$ through $\alpha_5$ are obtained. The Matalab® code written for this purpose and for other sections of this work is available in the repository. The real-life measurements of process parameters in an automobile industry cannot be perfect and expected to involve random errors. Any conclusion based on assumption of data being correct may lead to erroneous conclusions or the real data may not fit in with the theoretical data at all. It is logical to believe that the values of the parameters with which the coefficient identification, $\alpha_1$ through $\alpha_5$ has been taken up in the previous step are not the absolute correct but erroneous data. To analyze the impact of such imperfection in measurements on identification of the coefficients; the measurement data are added with 1%, 2% and 5% Gaussian white noise to

**Table 2. Participation coefficients at different noise**

| Coefficient | Associated parameter | Measured Parameters condition | | | |
|---|---|---|---|---|---|
| | | Pure | 1% GWN | 2% GWN | 5% GWN |
| $\alpha_1$ | % NVM<br>*estimation error* | -0.5863<br>*nil* | -0.5552<br>*5.2952* | -0.6656<br>*-13.5259* | -0.4207<br>*28.2349* |
| $\alpha_2$ | Temperature<br>*estimation error* | 0.3874<br>*nil* | 0.3942<br>*-1.7596* | 0.3897<br>*-0.5874* | 0.4448<br>*-14.8060* |
| $\alpha_3$ | Process Time<br>*estimation error* | -0.0175<br>*nil* | -0.0174<br>*0.5959* | -0.0191<br>*-8.9256* | -0.0203<br>*-16.2588* |
| $\alpha_4$ | Voltage<br>*estimation error* | 0.1147<br>*nil* | 0.1127<br>*1.7381* | 0.1192<br>*-3.9144* | 0.1008<br>*12.1135* |
| $\alpha_5$ | Surface Area<br>*estimation error* | -0.2343<br>*nil* | -0.2374<br>*-1.3068* | -0.2312<br>*1.3093* | -0.2319<br>*1.0275* |

compensate for measurement errors. The results with the pure measurement data and noise added data are presented in Table 2.

The units of the 5 process parameters have been kept colloquial, so that the values registered are of the similar order. This consideration is important because all the matrix based mathematical operations are highly dependent on the order of the numerals forming the rows and columns. From the coefficients obtained from the pure measured values, the participation coefficients for %NVM, Process time and surface area are negative. In electrode-based coatings, these are naturally expected since greater concentration of NVM renders the movement of the particles lowered. The marginal value of coefficient for Process time indicates the fact that the sensible coating thickness is deposited in the initial phase itself and prolonging the duration does not help enhancement of coating thickness. Enhanced surface area essentially lowers the coating thickness, as seen in $\alpha_5$. However, these values of the coefficients have meaningful interpretation only in the combined parameter test. In case of single variable tests, %NVM, Temperature, process time and voltage are bound to register positive coefficients while surface area would register negative coefficient.

The matrix based least square regression algorithm developed and expressed as equation (4) and (6) were tested with noise added parameter values. The deviation of the estimated coefficients viz. $\alpha_1$ through $\alpha_5$ with noisy measurement data are presented in the subsequent columns of Table 2. It is observed that at 1% and 2% random noise added data, the coefficient estimates are close to the estimated coefficients with pure measured data. At random noise at 5% of the measured value, the coefficients deviate. Coefficient associated with % NVM appears to be the most affected coefficient in presence of measurement noise. Overall, the regression algorithm is robust in presence of marginal measurement noise. Furthermore, with ISO and QS quality standards in place, measurement device accuracy and calibration are one of the main focuses in paint shops and a measurement error greater than 2% is probably not encountered. Thus, the algorithm is robust for application in physical paint shop.

Based on the results of the least square regression, therefore, the relationship of DFT with the operating parameters can be expressed as:

$$DFT = 0.1147\mathrm{V} + 0.3874\theta - 0.5863\rho + -0.0175\mathrm{t} - 0.2343A \quad (7)$$

Another 25 sets of experimental data are picked to test the validity of the coefficients obtained from the least square regression algorithm. These 25 sets are apart from the data used to establish the algorithm. The data used to test the validity of the algorithm is presented in Table 3.

The measured values of the parameters as recorded in Table 3 are used in equation (7) to validate, whether the experimentally obtained DFT matches with the DFT value predicted by the regression algorithm. The results of DFT values obtained with equation (7) are listed in the last column of Table 3. Since the DFT is measured in microns, actual measured values are significant only up to one place after decimal, the calculated values are not bound with

**Table 3. Data used for validation of the regression algorithm**

| % NVM | Temp. | Process Time | Voltage | S. Area | DFT | |
|---|---|---|---|---|---|---|
| | | | | | Measured | *Calculated* |
| 15.27 | 31.2 | 150 | 300 | 48 | 22.6 | 23.6659 |
| 15.27 | 31.2 | 150 | 300 | 48 | 23.5 | 23.6659 |
| 15.27 | 31.2 | 150 | 300 | 48 | 23.4 | 23.6659 |
| 15.27 | 31.2 | 150 | 320 | 48 | 28.1 | 25.9594 |
| 15.27 | 31.2 | 150 | 320 | 48 | 29.5 | 25.9594 |
| 15.27 | 31.2 | 150 | 320 | 48 | 28.8 | 25.9594 |
| 15.27 | 31.2 | 150 | 320 | 48 | 25.4 | 25.9594 |
| 15.27 | 31.2 | 150 | 320 | 48 | 27.4 | 25.9594 |
| 15.27 | 31.2 | 150 | 340 | 48 | 36.8 | 28.2529 |
| 15.27 | 31.2 | 150 | 340 | 48 | 37.1 | 28.2529 |
| 15.27 | 31.2 | 150 | 340 | 48 | 38.3 | 28.2529 |
| 15.27 | 31.2 | 150 | 280 | 48 | 35.4 | 28.2529 |
| 16.00 | 30.0 | 150 | 280 | 48 | 20.1 | 20.4795 |
| 16.00 | 30.0 | 150 | 280 | 48 | 18.6 | 20.4795 |
| 16.00 | 30.0 | 150 | 280 | 48 | 19.9 | 20.4795 |
| 16.00 | 30.0 | 150 | 280 | 48 | 20.4 | 20.4795 |
| 16.00 | 30.0 | 150 | 280 | 48 | 21.5 | 20.4795 |
| 16.00 | 30.0 | 150 | 280 | 48 | 19.3 | 20.4795 |
| 15.21 | 30.0 | 180 | 280 | 48 | 24.8 | 20.4177 |
| 15.21 | 30.0 | 180 | 280 | 48 | 23.4 | 20.4177 |
| 15.21 | 30.0 | 180 | 280 | 48 | 22.6 | 20.4177 |
| 15.21 | 30.0 | 180 | 280 | 48 | 23.4 | 20.4177 |
| 15.21 | 30.0 | 180 | 280 | 48 | 22.3 | 20.4177 |
| 15.21 | 30.0 | 180 | 280 | 48 | 23.7 | 20.4177 |
| 15.21 | 30.0 | 160 | 280 | 48 | 21.1 | 20.4177 |

the physical limitations of measurement. So, the 4$^{th}$ place beyond decimal has been retained.

The % of deviation in calculated DFT on base reading of measured DFT has been quantified. Interestingly, though the measured DFT is the base for error calculation; this value itself is the main source of error in such experiments. As can be seen from the first 3 entries in the table – all process parameters are same, but records different DFT. Since the calculated value is based on same process parameter value – they are identically same. The average of error in calculated DFT on base line of measured DFT is -6.5809 %. This is in acceptable limits by all standards of paint shop standardization (because the lower and upper limit of accepted DFT is in the range of 16 to 23 μm). The effect of noise corruption of the process parameter data has been checked on the same procedure as above and the average of error in calculated DFT on base line of measured DFT is -7.18% at 5% Gaussian White Noise in the measured values of process parameters.

It is evident from analysis of the data that, the main source of error is the measurement error itself. Within limits of the measurements, the participation coefficient identification algorithm developed is robust to measurement noise. The inverse problem of predicting the DFT from the measured process parameters is also stable, up to 5%

noise. Equation (7) brings out some conclusions of practical importance. It appears better to alter the electrode voltage and bath temperature to control DFT compared to the processing time. Also, since the coefficient of %NVM in equation (7) has the largest magnitude (though negative, in the combined study), it will influence the DFT maximum. Therefore, the most economical way around would be to keep the bath chemistry intact and change the physical quantities viz. electrode voltage and bath temperature to obtain the most economical output. Therefore, the present work correlates process parameters with change in DFT and provides a straightforward theoretical model which can be used to optimize the process parameters to get superior paint quality with minimum possible cost.

## 4. Conclusion

A water-based epoxy-coated mild steel prepared through cathodic electro deposition method and computational modelling was carried out to optimize the process parameters for dry film thickness for achieving superior paint quality at minimum cost in an automotive plant. Dry film thickness of the coated mild steel was measured using DFT meter and found to be within accepted limits of the computed values. The regression model has been used to adjust various parameters such as electrode voltage, bath temperature, processing time, non-volatile matter, and surface area to optimize the dry film thickness. The average dry film thickness computed using the model were in the range of 15- 35 μm. The error in computed dry film thickness with reference to experimentally measured dry film thickness value is -0.5809%, which is well within the acceptable limits by all standards of paint shop standardization. Results show that dry film thickness on mild steel is more sensitive to electrode voltage and bath temperature compared to processing time. Further, since the coefficient of %NVM has the largest magnitude (though negative, in the combined study), it is expected to have maximum influence on dry film thickness. Therefore, the most economical way around would be to keep the bath chemistry intact and change the physical quantities viz. electrode voltage and bath temperature to obtain the most economical output.

## Acknowledgement

For this research paper I would like to acknowledge Mr. Pradeep K Gupta, DGM, Paint Factory, Tata Motors Ltd, Jamshedpur for his continuous support throughout the development of the regression model.

## References

1. N. Cliff, M. Kanouni, C. Peters, P. V. Yaneff, K. Adamsons, Use of reactable light stabilizers to prevent migration and to improve durability of coatings on plastic substrates, *JCT Research*, **2**, 371 (2005). Doi: https://doi.org/10.1007/S11998-005-0005-Y
2. J.Y. Lee, M.S. Yi, H.C. Jeong, J.T. Kim, J.H. Nam, S.M. Noh, H.W. Jung, Characterization of clearcoats containing phosphoric acid-functionalized acrylic polyols for automotive precoated metal sheet coatings, *Journal of Coatings Technology and Research*, **11**, 697 (2014). Doi: https://doi.org/10.1007/S11998-014-9589-4
3. A.E. Matthews, G.M. Davies, Precoated Steels Development for the Automotive Industry, *Proc. IMechE Part D: Journal of Automobile Engineering*, **211**, 319 (1997). Doi: https://doi.org/10.1243/0954407971526461
4. M.D. Soucek, Z. Zong, A.J. Johnson, Inorganic/organic nanocomposite coatings: The next step in coating performance, *JCT Research*, **3**, 133 (2006). Doi: https://doi.org/10.1007/S11998-006-0016-3
5. R.A. Dickie, D.R. Bauer, S.M. Ward, D.A. Wagner, Modeling paint and adhesive cure in automotive applications, *Progress in Organic Coatings*, **31**, 209 (1997). Doi: https://doi.org/10.1016/S0300-9440(97)00039-8
6. M. M. L. Elahi, Modeling And Simulation Of A General Motors Conveyor System Using A Custom Decision Optimizer, The University of Texas at Arlington (2008). https://rc.library.uta.edu/uta-ir/bitstream/handle/10106/1869/Elahi_uta_2502M_10132.pdf?sequence=1&isAllowed=y
7. B. Schneider, A. Drews, M. Jagner, S.J. Simko, J.L. Tardiff, Characterization of zirconium oxide-based pretreatment coatings part 2 - Challenges in coating aluminum body panels, *SAE International Journal of Materials and Manufacturing*, **2**, 425 (2009). Doi: https://doi.org/10.4271/2009-01-0892
8. M. Doerre, L. Hibbitts, G. Patrick, N.K. Akafuah, Advances in Automotive Conversion Coatings during Pretreatment of the Body Structure: A Review, *Coat-*

*ings*, **8**, 405 (2018). Doi: https://doi.org/10.3390/COATINGS8110405

9. P. Couture, C. Blaise, D. Cluis, C. Bastien, Zirconium toxicity assessment using bacteria, algae and fish assays, *Water Air and Soil Pollution*, **47**, 87 (1989). Doi: https://doi.org/10.1007/BF00469000
10. P. Deshpande, A. Kolekar, Impressed Current Cathodic Protection of Low Carbon Steel in Conjunction with Conducting Polyaniline based Paint Coating, *Protection of Metals and Physical Chemistry of Surfaces*, **55**, 1236 (2019). Doi: https://doi.org/10.1134/S2070205119060078
11. S. Rossi, M. Fedel, L. Da Col, F. Deflorian, S. Petrolli, Coatings to increase the corrosion behaviour of aluminium foam, *Surface Engineering*, **33**, 405 (2017). Doi: https://doi.org/10.1080/02670844.2016.1276700
12. N.K. Akafuah, S. Poozesh, A. Salaimeh, G. Patrick, K. Lawler, K. Saito, Evolution of the Automotive Body Coating Process—A Review, *Coatings*, **6**, 24 (2016). https://doi.org/10.3390/COATINGS6020024
13. L.S. Cavalcante, V.S. Marques, J.C. Sczancoski, M.T. Escote, M.R. Joya, J.A. Varela, M.R.M.C. Santos, P.S. Pizani, E. Longo, Synthesis, structural refinement and optical behavior of $CaTiO_3$ powders: A comparative study of processing in different furnaces, *Chemical Engineering Journal*, **143**, 299 (2008). Doi: https://doi.org/10.1016/j.cej.2008.05.017
14. M. Choikhrue, S. Prombanpong, P. Sriyotha, An Effect of Coating Parameters to Dry Film Thickness in Spray Coating Process, *Key Engineering. Materials*, **709**, 95 (2016). Doi: https://doi.org/10.4028/WWW.SCIENTIFIC.NET/KEM.709.95
15. V.A. and D.V. Lamb, Physical and Mechanical Properties of Electrodeposited Copper, *Plating*, **52**, 1289 (1965).
16. K. Subramanian, V. M. Periasamy, M. Pushpavanam, K. Ramasamy, Predictive Modeling of Copper in Electrodeposition of Bronze Using Regression and Neural Networks, *Portugaliae Electrochimica Acta*, **27**, 47 (2009). Doi: https://doi.org/10.4152/pea.200901047
17. R. Balaji, M. Pushpavanam, K. Yogesh Kumar, K. Subramanian, Electrodeposition of bronze-PTFE composite coatings and study on their tribological characteristics, *Surface and Coatings Technology*, **201**, 3205 (2006). Doi: https://doi.org/10.1016/j.surfcoat.2006.06.039
18. N.U. Ramanathan K., Periasamy V. M., Malathy, Pushpavanam, Prediction of volume fraction of diamond deposition in Ni-diamond composite coatings – An artificial neural network approach-Indian Journals, *Journal of Metallurgy and Materials Sciemce*, **50**, 57 (2008). Doi: https://www.indianjournals.com/ijor.aspx?target=ijor:jmms&volume=50&issue=1&article=006 (accessed November 22, 2021).